ELSEVIER

Contents lists available at ScienceDirect

Materials Science & Engineering A

journal homepage: www.elsevier.com/locate/msea



Workhardening and the microstructural characteristics of shot- and laser-peened austenitic stainless steel



Masayoshi Kumagai ^{a,*}, Koichi Akita ^b, Muneyuki Imafuku ^a, Sin-ichi Ohya ^a

- ^a Department of Mechanical Systems Engineering, Tokyo City University, 1-28-1 Tamazutsumi, Setagaya-ku, Tokyo 158-8557, Japan
- ^b Quantum Beam Science Directorate, Japan Atomic Energy Agency, 2-4 Shirakata, Tokai-mura, Ibaraki-prefecture 319-1195, Japan

ARTICLE INFO

Article history: Received 20 February 2014 Received in revised form 11 April 2014 Accepted 16 April 2014 Available online 30 April 2014

Keywords:
Peening
Austenitic stainless steel
Workhardening
Hardness
Dislocation density
X-ray diffraction

ABSTRACT

The mechanical properties of shot- and laser-peened austenitic stainless steels, AISI316, were evaluated via Vickers hardness tests, and the correlation between workhardening and microstructural characteristics were discussed. Dislocation density, which is a microstructural feature, was determined via X-ray line profile analysis. Martensite was generated only by the shot-peening process. A linear relationship is observed between the hardness and the square root of the dislocation density in spite of the martensite formation on the shot-peened specimen. Therefore, the hardness is increased only by workhardening and is not affected by the martensite. We also clarified that a compressive residual stress greater than the original yield strength of the bare material can be induced because of the increase in yield strength caused by workhardening due to dislocation density increase with the peening process.

© 2014 Elsevier B.V. All rights reserved.

1. Introduction

Peening is a surface treatment technique to induce compressive residual stress on the surface of materials to improve their mechanical properties or corrosion resistance. Shot peening (SP) and laser peening (LP) are common peening techniques used in industry. SP is widely used on numerous types of mechanical parts, including springs, bearings, and gears. LP is used mainly on welded parts for nuclear power plants [1] and mechanical components of aircrafts [2]. For both SP and LP, compressive residual stresses are introduced by plastic deformation of the surface layer due to mechanical force; however, the energy sources are completely different. In SP, the energy source is provided by the impact of a surface with shot media such as small particles of metal, glass, and ceramics [3], while in LP it is provided by plasma shock waves generated by irradiation of laser pulses with sufficient energy [1,4].

Therefore, although the same residual stresses are induced in materials, their microstructures and mechanical properties may differ. Understanding the differences in the microstructural and mechanical features induced by different peening techniques is useful in the development of advanced peening techniques and their appropriate applications.

Dislocations are a critical determinant of the mechanical properties, and the increase in dislocation density induces work-hardening. Kumagai et al. [5,6] studied the microstructures of specimens subjected to SP and LP by X-ray line profile analysis (LPA). LPA can be used for the quantitative analysis of materials rather than transmission electron microscopy, and the information thus obtained is useful in evaluating the relationships between microstructural characteristics and mechanical properties.

In this study, we investigated the mechanical properties of both SP and LP specimens and discussed the correlation between workhardening and microstructural characteristics analyzed using LPA. In addition, since it was shown that martensite transformation occurs only in the SP specimen [5,6], we also studied the influence of martensite (α '-Fe) on the hardness of the specimen.

2. Experimental

Austenitic stainless steel, AlSI316, was used for the experiments; the chemical composition of the specimen used in this study is shown in Table 1. The as-received materials were solution heat treated at 1050 °C for 1 h in air and then quenched in water. Stress relief annealing was subsequently performed at 600 °C for 0.5 h under vacuum. The mechanical properties of the heat-treated material (bare material)—the 0.2% proof stress (yield strength) was 291 MPa, the tensile stress was 626 MPa, and the Young's modulus was 199 GPa— were obtained via tensile test.

^{*} Corresponding author: Tel: +81 3 5707 0104. E-mail address: mkumagai@tcu.ac.jp (M. Kumagai).

Table 1 Chemical composition of the material.

С	Si	Mn	P	S	Ni	Cr	Мо
0.1	0.4	0.8	0.3	0	10	16	2.1

Shot and laser peening were performed on the bare materials. In the SP process, the shot media, which was cut-wire made of 430 stainless steel wires of diameter 0.6 mm, was bombarded at a pressure of 0.5 MPa with a peening coverage of 300%. In the LP process, a pulsed Q-switched Nd: YAG laser oscillator with a second harmonic generator was used to irradiate laser beam onto the uncoated bare material in a water pool. The laser wavelength was 532 nm, the pulse energy was 20 mJ, the pulse duration was 8 ns, the spot diameter was 0.3 mm, and the coverage was 1270%. In order to compare the microstructural characteristics and mechanical properties of the specimens subjected to two different peening techniques, conditions that can result in similar residual stress profiles in the depth direction were selected. The specimens were the same as those used in the previous studies [5,6].

Residual stresses were measured via the $\sin^2\!\psi$ method [7], a common X-ray stress measurement method. Residual stress profiles in the depth direction were obtained by repeating the X-ray stress measurements and electrochemical polishing. An Mn–K α X-ray source was used. The diffraction index was 311 for austenite (γ -Fe). The X-ray stress constant was -302 MPa/deg, which was calculated using the Kroner model with single-crystal elastic stiffness (C_{11} =206 GPa, C_{12} =133 GPa, and C_{44} =119 GPa) [8]. The measurement range of $\sin^2\!\psi$ was 0–0.6 at intervals of 0.1.

Vickers hardness tests were performed to determine the hardness of the specimens as a typical value of their mechanical properties. The indentation load was 0.981 N, and the loading time duration was 15 s; five tests were performed on each sample.

X-ray diffraction line profiles were measured at seven arbitrary depths from the original surface to approximately 300 μ m using an X-ray diffractometer with Bragg–Brentano geometry. The X-ray measurement and electrochemical polishing were performed repeatedly. Cu-K α X-rays were used; whole line profiles from 40° to 100° were measured and four individual indices (i.e., 111, 200, 220, and 311) of γ -Fe were precisely measured. Modified Williamson–Hall/Warren–Averbach methods [9,10] were employed for LPA, and the dislocation densities of γ -Fe in the specimens were obtained. The LPA procedure has been shown in the previous articles [5,6].

3. Results

3.1. Residual stress and hardness

The residual stress distributions of the SP and LP specimens, which have been previously reported [5], are shown in Fig. 1. The values show the averaged residual stresses in two orthogonal directions. The residual stresses on the original surfaces of the SP and LP specimens were -561 and -653 MPa, respectively. Although the stress of the SP specimen was slightly higher than that of the LP specimen, the stress distributions were approximately the same. The compressive residual stresses of both specimens increased with increasing depth from the surface and reached their maximum values at a depth of approximately 50 μm in both cases. The compressive residual stresses decreased with increasing depth at $> 50 \,\mu m$ and became approximately -200 MPa at a depth of $400-500 \,\mu\text{m}$ in both specimens. The residual stress of the bare material was approximately -200 MPa; therefore, the induced depth of the residual stress was approximately 400 µm.

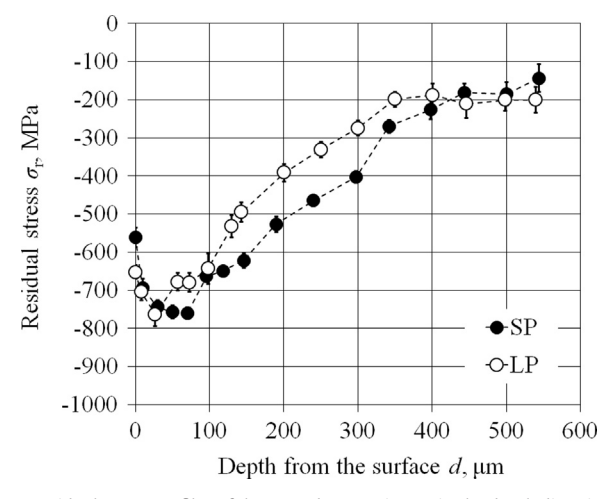


Fig. 1. Residual stress profiles of the SP and LP specimens in the depth direction [5].

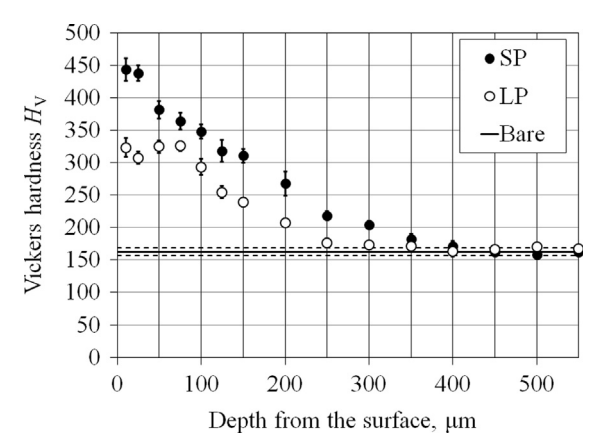


Fig. 2. Vickers hardness profiles of the SP and LP specimens in the depth direction. Dashed lines are standard deviations of hardness of the bare specimen.

Fig. 2 shows the Vickers hardness profiles of the SP and LP specimens in the depth direction. The hardness of the SP and LP specimens at the original surface were HV444 and HV323, respectively. The hardness of the bare specimen was HV163. The hardness of both specimens gradually decreased along the depth, and at 400–500 μ m, it became same as that of the bare specimen. In addition, the hardness of the SP specimen was greater than that of the LP specimen at all depths until the hardness became the same as that of the bare specimen.

3.2. Microstructural characteristics

Fig. 3 shows the whole line profiles of all the specimens. The 111, 200, 220, 311, and 222 reflections from γ-Fe were observed in the line profile of the bare specimen. In the line profile of the SP specimen, in addition to the γ-Fe peaks, several peaks (110, 200, 211, and 220) of α′-Fe, were observed. The presence of these peaks indicates that γ-Fe transformed into α′-Fe during the SP process and that α′-Fe was present in the specimen. This result indicates that the SP process caused deformation-induced martensite transformation. In the case of the line profile of the LP specimen, peaks attributable to γ-Fe only were observed. Martensite transformation did not occur in the case of the sample subjected to LP, in contrast to the sample subjected to SP. The whole line profiles of the SP specimen at each depth were also evaluated. Fig. 4 shows the whole line profiles of the SP specimen at several depths from the original surface. With increasing depth, the peak intensities of α′-Fe decreased and the

Download English Version:

https://daneshyari.com/en/article/1575087

Download Persian Version:

https://daneshyari.com/article/1575087

<u>Daneshyari.com</u>